171
3/8/80

DR-658

ornl

OAK
RIDGE
NATIONAL
LABORATORY

UNION
CARBIDE

OPERATED BY
UNION CARBIDE CORPORATION
FOR THE UNITED STATES
DEPARTMENT OF ENERGY

ORNL-5606

The Irradiated-Microsphere Gamma Analyzer (IMGA)—An Integrated System for HTGR Coated Particle Fuel Performance Assessment

M. J. Kania
K. H. Valentine

MASTER

ORNL-5606
Distribution
Category UC-77

Contract No W-7405-eng-26

METALS AND CERAMICS DIVISION

HTGR BASE TECHNOLOGY PROGRAM

Fueled Graphite Development (189a 01330)

THE IRRADIATED-MICROSPHERE GAMMA ANALYZER (IMGA) — AN INTEGRATED SYSTEM FOR HTGR COATED PARTICLE FUEL PERFORMANCE ASSESSMENT

M. J. Kania and K. H. Valentine

Date Published: February 1980

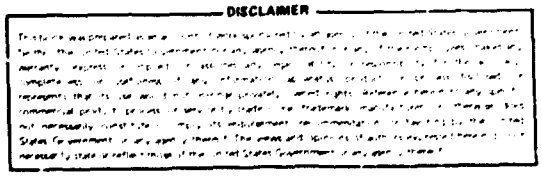

OAK RIDGE NATIONAL LABORATORY
Oak Ridge, Tennessee 37830
operated by
UNION CARBIDE CORPORATION
for the
DEPARTMENT OF ENERGY

CONTENTS

THE IRRADIATED-MICROSPHERE GAMMA ANALYZER (IMGA) — AN INTEGRATED SYSTEM FOR HTGR COATED PARTICLE FUEL PERFORMANCE ASSESSMENT

M. J. Kania and K. H. Valentine*

ABSTRACT

The Irradiated-Microsphere Gamma Analyzer (IMGA) System, designed and built at ORNL, provides the capability of making statistically accurate failure fraction measurements on irradiated HTGR coated particle fuel. The IMGA records the gamma-ray energy spectra from fuel particles and performs quantitative analyses on these spectra; then, using chemical and physical properties of the gamma emitters it makes a failed-nonfailed decision concerning the ability of the coatings to retain fission products. Actual retention characteristics for the coatings are determined by measuring activity ratios for certain gamma emitters such as $^{137}Cs/^{95}Zr$ and $^{144}Ce/^{95}Zr$ for metallic fission product retention and $^{134}Cs/^{137}Cs$ for an indirect measure of gaseous fission product retention.

Data from IMGA (which can be put in the form of n failures observed in N examinations) can be accurately described by the binomial probability distribution model. Using this model, a mathematical relationship between IMGA data (n,N), failure fraction, and confidence level was developed. To determine failure fractions of less than or equal to 1% at confidence levels near 95%, this model dictates that from several hundred to several thousand particles must be examined. The automated particle handler of the IMGA system provides this capability. As a demonstration of failure fraction determination, fuel rod C-3-1 from the OF-2 irradiation capsule was analyzed and failure fraction statistics were applied. Results showed that at the 1% failure fraction level, with a 95% confidence level, the fissile particle batch could not meet requirements; however, the fertile particle exceeded these requirements for the given irradiation temperature and burnup.

1. INTRODUCTION

Coated-particle fuel[1,2] for High-Temperature Gas-Cooled Reactor (HTGR) application is designed such that each fuel particle has its own primary containment vessel. This containment is in the form of multiple coatings on a spherical fuel kernel. Two commonly used designs are the Biso- and

---

*Instrumentation and Controls Division.

Triso-coatings. The Biso-coating is a two-layer coating consisting of a porous inner layer of a low-density carbon surrounded by a high-density isotropic pyrocarbon outer layer. The Triso-coating is a four-layer coating with the first two layers similar to the Biso-coating (except for thicknesses) followed by a layer of SiC and another layer of high-density isotropic pyrocarbon.

A commercial HTGR core would nominally require 10^9 to 10^{11} individual coated particles. Either type of particle or a mixture of both might be stipulated. With this large number of coated particles it is important to verify that fission product losses through defective or broken coatings will be kept to an acceptable minimum. Accordingly, fuel-performance specifications[3] have been based on the expected fission product releases from failed fuel over the HTGR core life. These performance specifications set rigid standards to qualify a candidate fuel for HTGR use. The standards, which dictate limits on the amount of gaseous and metallic fission product release for safe operation, can be translated into a failure fraction applicable to the irradiation performance[4] of the candidate fuel. Here, failure fraction is defined as the fraction of fuel that has lost a significant amount of its fission products through broken or defective coatings.

This report describes in detail the Irradiated-Microsphere Gamma Analyzer System[5,6] (IMGA), which was designed, built, and put into routine operation at Oak Ridge National Laboratory (ORNL). This system has the primary purpose of providing a statistically accurate measure of the failure fraction for irradiated coated-particle fuel. It has been shown to be reliable, accurate, and efficient.

2. DESCRIPTION OF IMGA SYSTEM

The Irradiated-Microsphere Gamma Analyzer system provides the capability of making statistically accurate measurements of failed particle fractions from irradiated HTGR fuel. Basically, IMGA consists of a high-resolution gamma-ray detector, a minicomputer-based pulse-height

analyzer, an automated particle handler, and appropriate interfaces to establish communication links between the three components. Each of the major components is described below:

Automated Particle Handler — The automated particle handler is the unique component of the IMGA system. It consists of three parts: a particle singularizer, which can select one or several irradiated coated particles from a large population and load them into a sample holder; a sample changer, which contains three sample holders, 120° apart, and rotates them from the load position to the detector position and finally to the drop position; and a particle collector, which contains 20 bins in which particles can be classified according to their respective radioisotopic analyses. Figure 1 shows the automated particle handler in position inside the IMGA hot-cell cubicle.

Pulse-Height Analyzer System — The pulse-height analyzer is a Tennecomp Systems, Inc., model TP-5000,* which is supplied with a Digitial Equipment Corporation model PDP-11/05 minicomputer. The PDP-11/05 is a 16-bit machine with 4096 (4K) 14-bit words of memory in the main frame. Three additional 8K memory extension modules yield a total of 28K words of storage. This memory is used for storage of programming and variables and a histogram region. Two mass storage devices are also available: A Digital Equipment Corporation model RK05 disk unit and a Tennecomp Systems DataPacer with two four-track data cartridge transports.

Gamma-Ray Detector — The gamma-ray detector used with the IMGA system is an ORTEC high-resolution lithium-drifted germanium, Ge(Li), detector. Coupled with the detector are pulse processing units consisting of an ORTEC model 120-4 preamplifier, an ORTEC model 472 main amplifier, and a Northern Scientific model NS 623 analog-to-digital converter (ADC). Figure 2 shows the Ge(Li) detector in the detector port of the IMGA cubicle.

These three components and their interfacing have been integrated into a sophisticated and versatile system. The automated particle handler has been installed in a shielded cubicle on the second level of the

*Trademark of Tennecomp Systems, Inc.

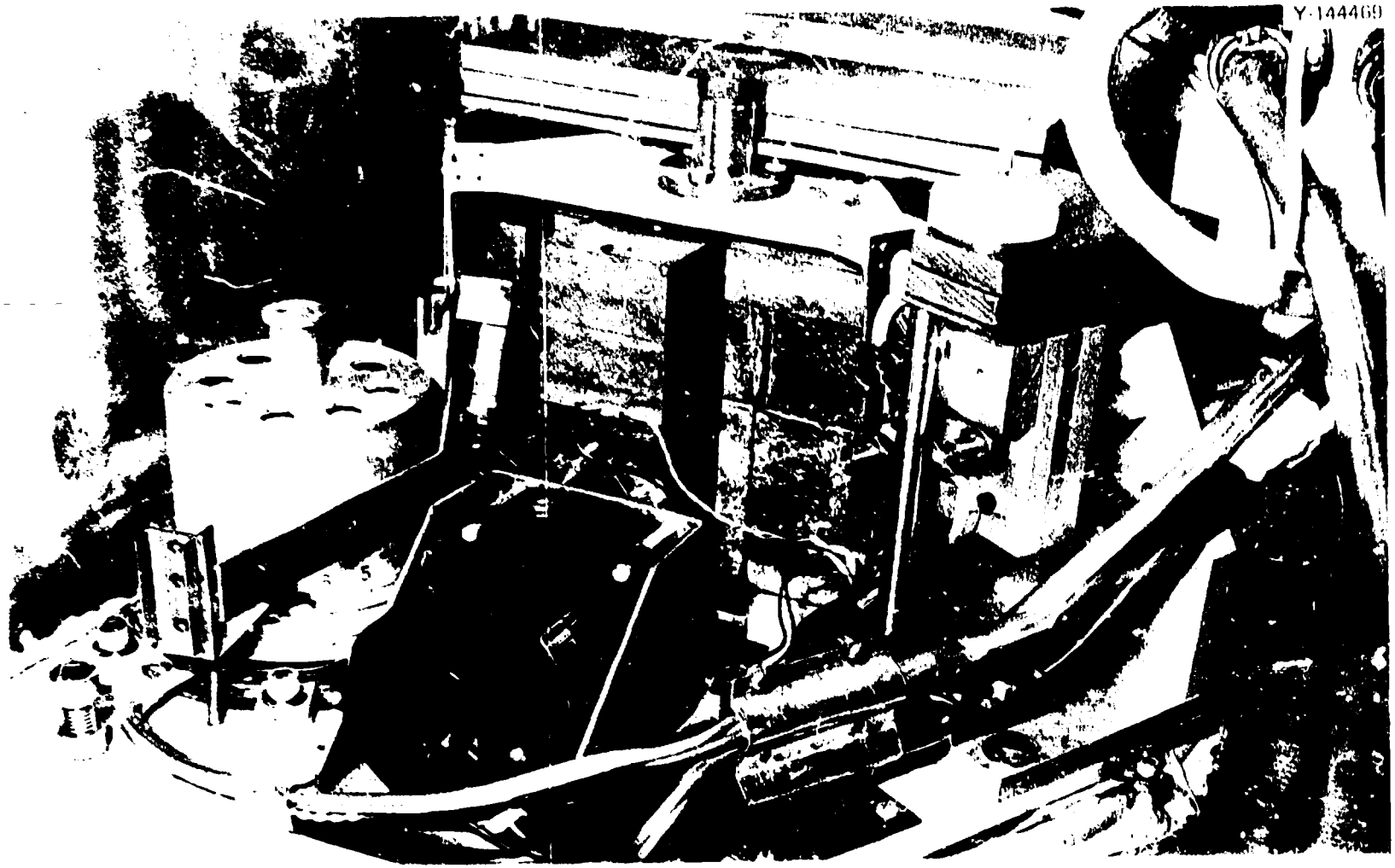

Fig. 1. Automated Particle Handler Positioned Inside IMCA Hot Cell Cubicle with its Gamma Shielding, Computer Interfacing, Vacuum and Pressure Lines.

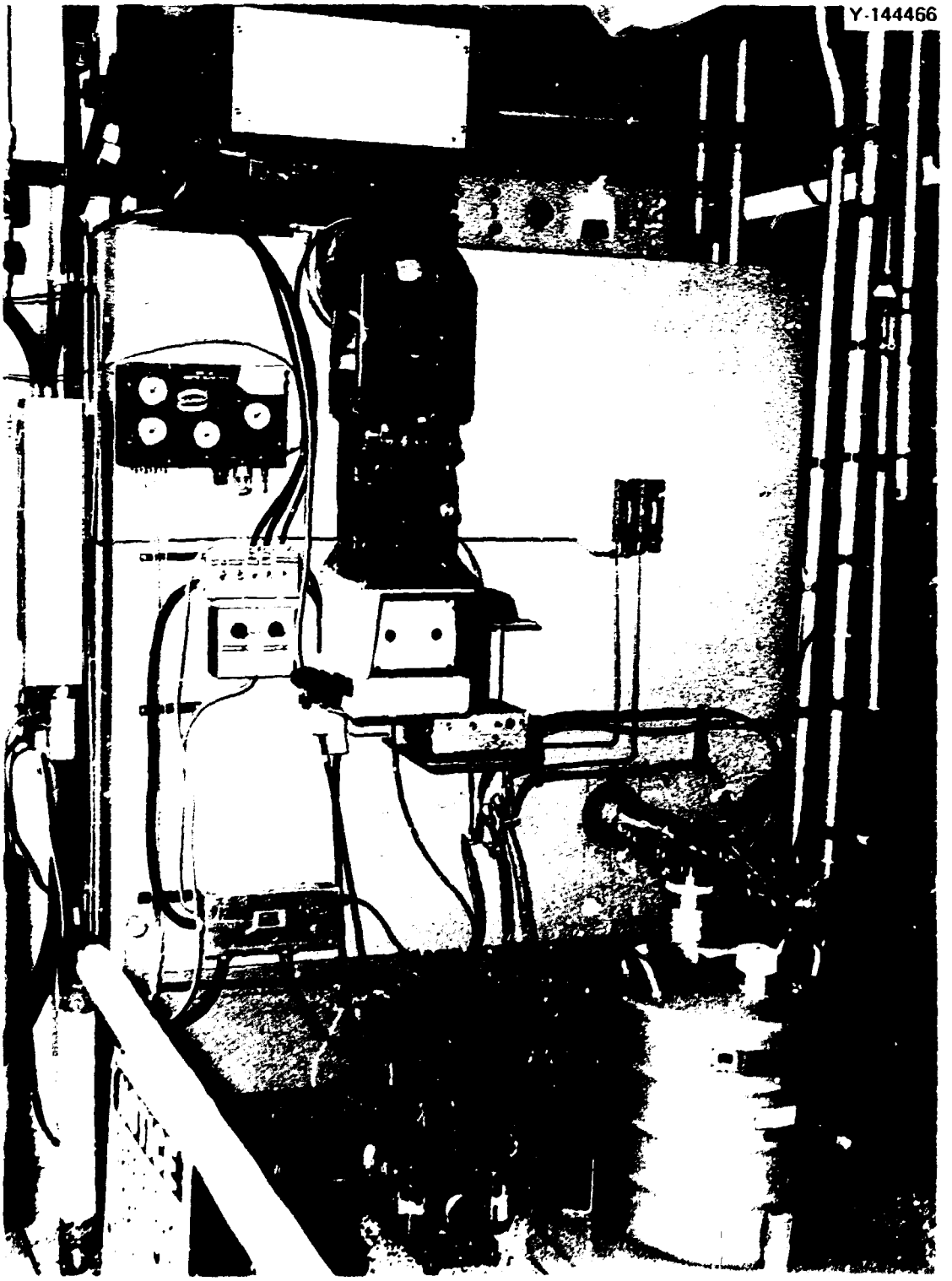

Fig. 2. Outside View of the IMGA Hot Cell Cubicle. Shown are the Ge(Li) gamma-detector in position and the external portion of the stereomicroscope.

High-Radiation-Level Examination Laboratory (HRLEL) at ORNL. The cubicle is positioned directly above the main hot-cell area on the first level. A transfer device from the main cell area to the IMGA cubicle enables irradiated coated particle fuel to be inserted into the cubicle without being removed from the air lock of the hot cells.

In addition to the handler, the IMGA cubicle contains a shielded stereomicroscope and a movable stage. This system, equipped with micromanipulators for single particle handling, is shown in Fig. 3. This device has been extremely useful in the handling of individual particles, kernels, and coating fragments. The movable stage has x, y, and z movement as well as full 360° rotation in the horizontal plane. The micromanipulator uses a vacuum sucti system to pick up objects and can rotate them a full 360° in the verticle plane. Three microscope objectives provide 10, 20, and 50× magnification and can be easily changed from one magnification to another inside the cubicle. A camera is built into the external portion of the microscope.

A scanning electron microscope (SEM) is attached to the back of the IMGA cubicle. This system can be used for detailed high-magnification examinations of particle surfaces, kernels, or coating fragments after IMGA examination and analysis.

3. FAILURE FRACTION MEASUREMENTS

In the past 20 years of coated particle fuel development[3,7-10] the primary goal has been to manufacture and qualify a fuel for HTGR application. Extensive irradiation programs have been conducted in real and accelerated time to develop coated particle fuels that will retain fission products. Analysis of the irradiation experiments has shown that both Triso- and Biso-coated particles are capable of retaining fission products.

3.1 Requirements and Measuring Techniques

Failure fraction determination is a complicated statistical process. Factors that contribute to the difficulty in making statistically significant measurements are:

Fig. 3. Stereomicroscope Objectives Along with Movable Stage for Single Particle Viewing and Handling. Microscope stage has x, y, and z movement along with full 360° rotation.

1. statistically meaningful results require examination of large numbers of particles (see Sect. 4.2) to place high confidence on measurement.
2. examination of large numbers of irradiated fuel particles requires sophisticated hot-cell facilities;
3. with failure fractions in the range from 10^{-2} to 10^{-4} the misclassification of one or two particles out of thousands can lead to large errors in the failure fraction measurement;
4. induced particle failure during normal postirradiation examination (PIE) procedures can lead to an erroneously large failure fraction when determined by destructive tests or heating experiments;
5. the failure fraction measurement must be independent of coated particle type and of specific failure mechanism.

To verify good irradiation performance we needed to develop techniques to measure particle failure fractions. These techniques have evolved and become more sophisticated as the level of knowledge of particle failure mechanisms[11,12] has increased. Methods that are most commonly used today for failure fraction measurements are listed below:

1. visual inspection of loose particles and polished metallographic cross sections of fuel rods (PIE procedure),
2. fission gas release-to-birth rate ratios (R/B values) on loose particles and fuel rods (in-situ as well as PIE procedure) — extension to gas content measurements of loose particles (PIE procedure),
3. hot gaseous chlorine leach measurements on loose particles and fuel rods (PIE procedure),
4. high-temperature annealing tests on loose particles and fuel rods (PIE procedure),
5. gamma spectroscopy on loose particles and fuel rods (PIE procedure),
6. microradiography of loose particles and small fuel rods (PIE procedure).

None of the methods listed totally satisfy all the requirements for a statistically significant measurement.

3.2 Measuring Failure Fractions with IMGA

Failure fraction determinations with IMGA are possible because of the high gamma-emission rates from fission products within an irradiated fuel particle. Figure 4 is a portion of the gamma-ray energy spectrum, 8 to 130 fJ (50–800 keV), obtained from one UC_2 particle irradiated in the Peach Bottom HTGR. The IMGA system measures such a gamma-ray spectrum for each fuel particle examined. A subsequent quantitative analysis of selected gamma peaks within the spectrum, along with knowledge of the physical and chemical properties of the fission products, allows an accurate assessment of irradiation performance.

The actual failure fraction measurement is based on fission-product retention and is made possible by the different volatilities of various fission and activation products in the fuel. By taking a ratio of the activity of a volatile fission product to a nonvolatile fission product, a measure of fission products released during irradiation can be obtained. An attractive feature of the ratio determination is its insensitivity to variations in the kernel size and heavy-metal loading.

Two isotopes of cesium (^{134}Cs and ^{137}Cs) and ^{95}Zr are of particular interest; all three emit easily detectable gamma rays in the 100 to 130 fJ (600–800 keV) range. In the high-temperature environment of the HTGR, cesium with a boiling point of 678°C will diffuse or escape much more readily from a defective coating than zirconium with a boiling point of 4377°C. Thus a measurement of the activity ratio of ^{137}Cs to ^{95}Zr can provide a measure of the retention of the metallic fission product cesium within the particle.

The ^{134}Cs isotope is not a direct fission product but rather an activation product produced by the reaction $^{133}Cs(n,\gamma)^{134}Cs$. The stable isotope of cesium, ^{133}Cs, is a fission product with a very low direct fission yield, <0.001%. However, the cumulative yield from ^{235}U fission is about 6.6%. The decay scheme for fission products with mass of 133, shown in Fig. 5, indicates that virtually all stable cesium inventory is a result of ^{133}Xe decay. (Numbers underlined in Fig. 5 are cumulative percent yields for ^{235}U fission.) Xenon-133 is a fission gas with a cumulative fission yield of about 6.6%. An activity measurement of ^{133}Xe

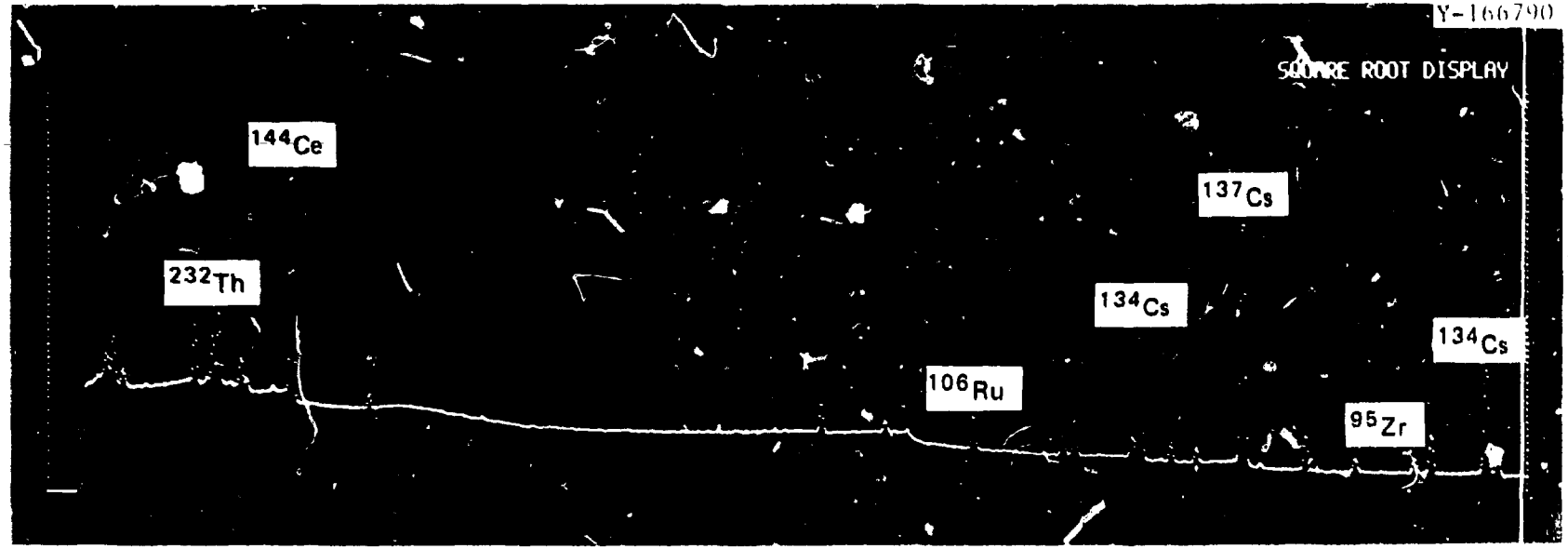

Fig. 4. Portion of the Gamma-Ray Energy Spectrum, 8 to 130 fJ (50–800 keV), Obtained from One UC_2 Particle Irradiated in the Peach Bottom HTGR. The capability of selecting gamma peaks of importance from the total gamma spectrum reduces IMGA examination and analysis time.

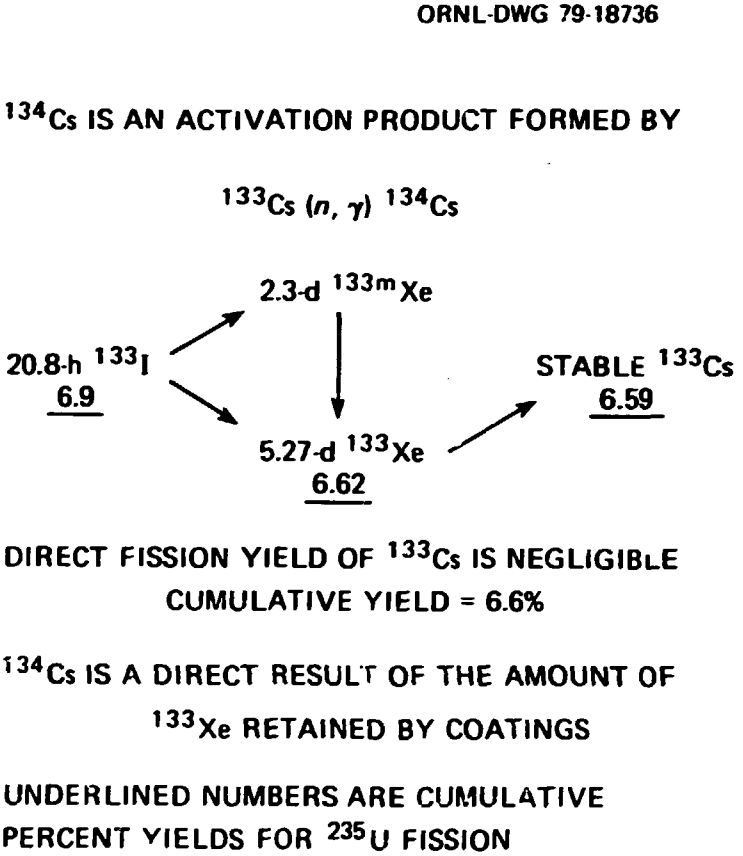

Fig. 5. The Activation Product ^{134}Cs May be Indicative of Fission Gas Content in HTGR Coated Particle Fuel. It is produced by an (n,γ) reaction of the stable isotope of cesium, which is a decay product of the fission gas ^{133}Xe.

($t_{1/2}$ = 5.2 d) is generally not possible because it has decayed to insignificance by the time postirradiation examinations have begun. However, ^{134}Cs has a relatively long half-life, 2.06 years. It can be directly related to the amount of ^{133}Cs and thus indirectly to the amount of ^{133}Xe retained by the particle. Therefore, a measurement of the activity ratio of ^{134}Cs to ^{137}Cs can provide an indirect measure of the particle's ability to retain fission gases. Particles broken during irradiation have reduced ^{134}Cs/^{137}Cs ratios because of the early loss of ^{133}Xe.

The two isotopes of cesium can also provide information about handling-induced failures that result from the routine processing during PIE. This type of failure usually results in the coating being broken off of the particle. When this occurs the resulting kernel in the population

used for the failure fraction measurement will be determined to be failed by the $^{137}Cs/^{95}Zr$ and $^{134}Cs/^{95}Zr$ activity ratios. This is due to the percentage of cesium that resides in the coatings of irradiated fuel and the large amount of zirconium that remains within the kernel. Such induced failures can be detected by consideration of the $^{134}Cs/^{137}Cs$ activity ratio coupled with visual and metallographic examination of the kernels. This procedure is valid only if the fission product inventory or distribution has not been altered from its state before PIE. Such changes can result when particles are tested by postirradiation annealing. In the case where no alteration of inventory has taken place, the $^{134}Cs/^{137}Cs$ activation ratio should be the same, even though the coating had been broken off, as in those particles with intact coatings. This is because the ratio in the kernel will remain constant.

For particles having carbide kernels it is important to consider the retention of the rare-earth fission products.[7,13] This is easily accomplished by monitoring the activity ratio of the fission products $^{144}Ce/^{95}Zr$.

3.3 Operation of Automated Particle Handler

Any conventional high-resolution gamma spectrometry system could be used to make the ratio measurements for small numbers of particles. However, statistical considerations dictate that from several hundred to several thousand particles be examined to accurately determine the failure fraction of a multi-particle sample. This would be almost impossible if each particle had to be handled individually but is a relatively simple task for IMGA.

Figure 6 is a diagram of the system showing the handler located within the IMGA cubicle. Although the actual particle handler (see Fig. 2) diverges somewhat from that shown, the figure still illustrates the basic functions of individual particle examinations. The sequential operation of the system is as follows:

1. A particle is loaded into the sample changer at position 1.

2. A 120° rotation of the sample changer aligns the particle with the Ge(Li) gamma detector. Data acquisition begins and a fission-product gamma spectrum is accumulated. The next particle is loaded at position 1.

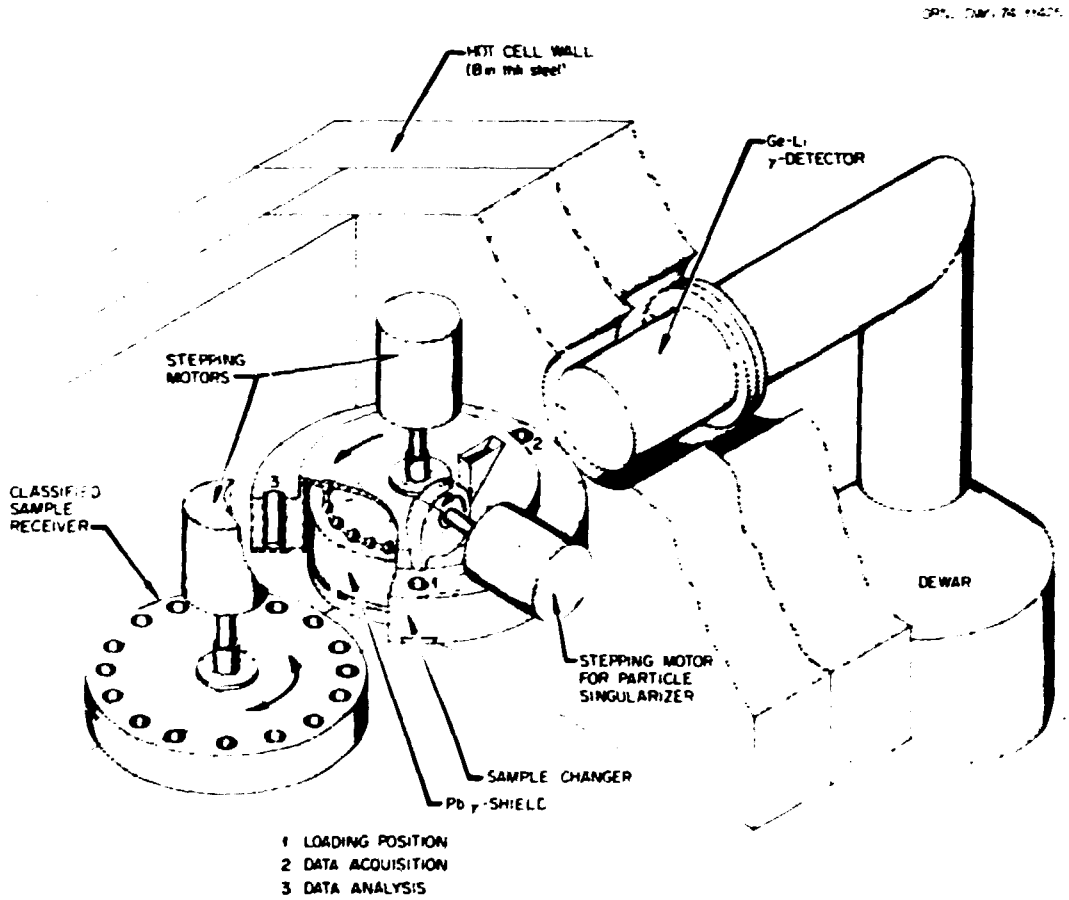

Fig. 6. Conceptional Design for the Irradiated Microsphere Gamma Annalyzer.

3. When the predetermined data acquisition time elapses, another 120° rotation of the sample changer aligns the next particle with the detector. The spectrum for the first particle is shifted to another part of the core memory and data acquisition is again initiated. After loading the third particle at position 1, the central processor (CPU) is free to analyze the spectrum of the first particle, which now resides at position 3.

4. Using results of the spectrum analysis, the CPU makes a logical decision and aligns one of the 20 bins of the particle collector under position 3 of the sample changer. At this point the particle in question has been classified as inert, fissile, or fertile and fission-product retention characteristics have been determined. The particle is then released into the appropriate bin. A record of the analysis is written onto the mass storage device.

5. The cycle is repeated until interrupted by the operator or the analysis is completed.

A single 120° rotation of the sample changer, including all operations directed by the CPU, requires a minimum of 3.5 s. Depending on particle burnup and cooling time, realistic examination rates are of the order of one to ten particles per minute. The ability of IMGA to segregate particles according to selected fission-product gamma spectrum properties can be extremely useful for further postirradiation investigations on particle-failure mechanisms.

The IMGA system was designed to operate with loose coated particles. Therefore, bonded HTGR fuel rods must be deconsolidated before IMGA examination. An electrolytic deconsolidation procedure has been developed for HTGR fuel rods[14] and is presently being used for all irradiated fuel rods scheduled for IMGA examination and analysis.

4. STATISTICAL BASES FOR FAILURE FRACTION DETERMINATION[15]

Accurate measurement of the failure fraction of irradiated coated particle fuel is vital to the HTGR fuel development program. Because of the importance in establishing accurate and reliable fuel performance data, many techniques are presently being used (See Sect. 3.1 for list of commonly used techniques).

4.1 Limitations of Visual Inspection Technique

The techniques that are most widely used to determine failure fractions are expensive and have the least statistical significance. These techniques are visual inspection of loose particles or polished metallographic cross sections of irradiated fuel. A typical polished cross section of a 12.7-mm-diam fuel rod may contain 10 to 50 particles of interest. The total fuel-particle inventory of a typical experimental 12.7-mm-diam by 50.8-mm-long fuel rod ranges from 1000 to 8000, depending on irradiation facilities. If one is optimistic and assumes a sample population of 100 particles in a cross section, then Fig. 7 illustrates the relationship between what is observed for the sample and what can be inferred about the total population from those observations.

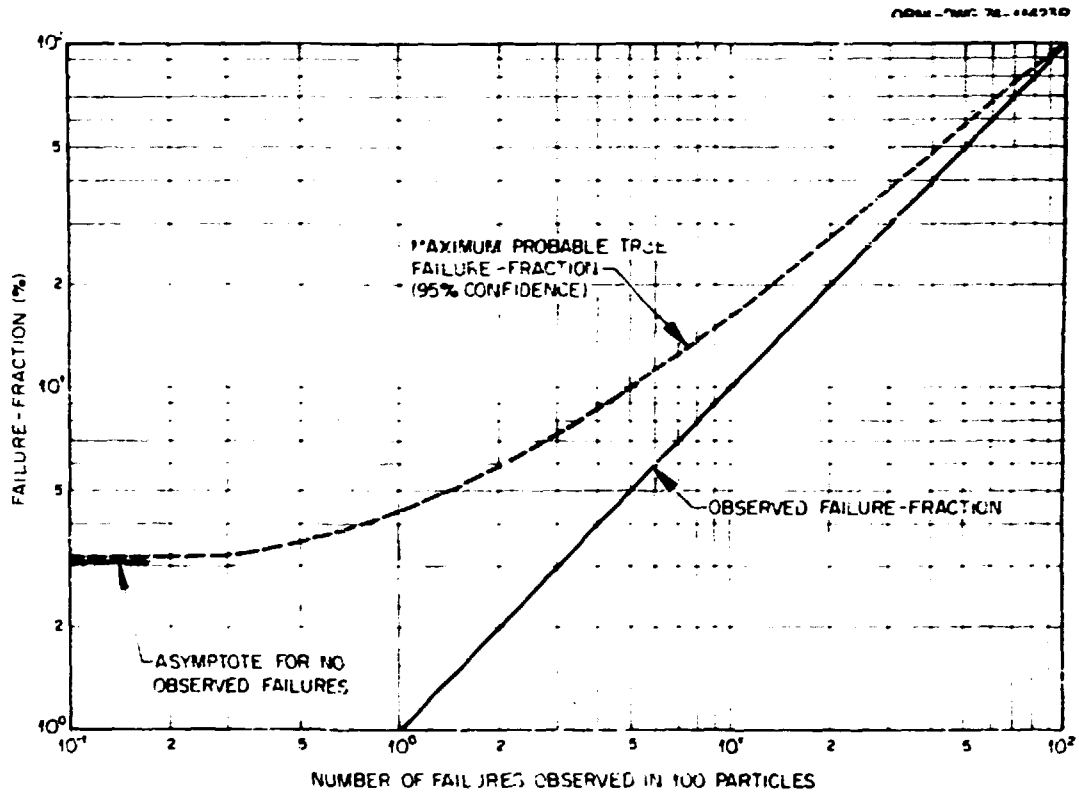

Fig. 7. Failure Fraction Determination from Examination of 100 Particles Produces Large Differences Between What is True for Sample Population and What is Likely True for the Total Fuel Population.

The solid line in Fig. 7 is a plot of the failure fraction against the number of observed failures. For example, one observed failure implies a failure fraction of 1%; likewise ten observed failures imply a failure fraction of 10%. These failure fractions are exact for the sample population in question. However, one must ask the question "How well does the observed failure fraction represent the total population failure fraction, and what is the confidence level of the estimate?" The dashed curve in Fig. 7 represents one of many possible answers to this question. It represents the locus of failure fraction values that are larger than the true failure fraction for the entire fuel rod* with 95% confidence.† Thus, if the observed failure fraction is 10% then one can be

*Based on the binomial probability distribution model and the assumption that the fuel rod contains an infinite population of particles.

†To make a statement with 95% confidence means that there is a 95% probability that the statement is true.

95% confident that the true value is less than 16.1%. Similarly, an observed failure fraction of 1% implies a true value that is less than 4.6%. However, even if no failures are observed one can be 95% certain only that the true value is less than 3.1%. In view of current design limits on fuel particle failure fractions of 1% to 0.01% at end-of-life (EOL), clearly many more than 100 particles must be examined.

4.2 Binomial Probability Distribution Model

Data from IMGA yield the number of failed particles, n, observed in N examinations. Here, n is a discrete binomial variable representing the number of observed failures. Thus, the probability of detecting n failures out of N examinations is given by the binomial probability distribution

$$P[n] = \frac{N!}{n!(N-n)!}\,\eta^n(1-\eta)^{N-n}\ , \tag{1}$$

where η is the true failure fraction of the total population. The ultimate aim is to establish an accurate estimate for η based on n and N. To establish this estimate we require answers to the previous questions, "How well does n/N represent the true failure fraction η?" and "With what confidence level does n/N approximate η?" Answers require a distribution over the continuous variable η. It follows then that the probability density function (pdf) for the continuous variable η is given by

$$\text{pdf} = \eta^n(1-\eta)^{N-n}/\int_0^1 \eta^n(1-\eta)^{N-n}d\eta\ . \tag{2}$$

In general, the probability that the failure fraction does not exceed a specified value of η is

$$P[n/N \leq \eta] = \frac{1}{B(j,k)}\int_0^{\eta} t^n(1-t)^{N-n}dt\ , \tag{3}$$

where

$$j = n + 1$$

$$k = N - n + 1$$

$B(j,k)$ = Complete beta function

$$= \int_0^1 t^{j-1}(1 - t)^{k-1} dt.$$

Conversely, the probability that the failure fraction is at least a specified value η is

$$P[n/N \geq \eta] = 1 - P[n/N \leq \eta] \ . \tag{4}$$

Equations (3) and (4) answer the first question, "How well does n/N represent the failure fraction η?" The second question, "With what confidence level does n/N approximate η?", can be answered by requiring that it have a confidence level of $C \times 100\%$. Applying this to Eqs. (3) and (4) means that there is a $100C\%$ probability that the statement is true. Therefore, the general equations that relate C, n, N, and η are

$$C = P[n/N \leq \eta] \ , \tag{5}$$

and

$$1 - C' = P[n/N \leq \eta] \ , \tag{6}$$

where C and C' are confidence coefficients and $P[n/N \leq \eta]$ is defined in Eq. (3).

Solutions to Eq. (5) for η yield a failure fraction of at least the true failure fraction with $C \times 100\%$ confidence. Solutions to Eq. (6) for η yield a failure fraction not exceeding the true failure fraction with $C' \times 100\%$ confidence. The solution for $P[N/n \leq \eta]$ is the incomplete beta function[16] defined as:

$$I_\eta(j,k) = 1 - (1 - \eta)^{j+k-1} \sum_{i=0}^{j-1} \binom{j + k - 1}{i} \left(\frac{\eta}{1 - \eta}\right)^i \ , \tag{7}$$

which can be solved by calculating points on the confidence curves. Figure 6 represents the confidence limits corresponding to a failure fraction of 1%. This figure illustrates the magnitude of the problem of demonstrating that a particular fuel satisfies the current design limit on fuel failure fraction. The curve labeled "95% confidence that failure fraction < 0.01" is similar to the curve of Fig. 7 except that in the present case the failure fraction is specified rather than the number of observed failures. Points on the lower curve represent conditions that must be satisfied to state with 95% confidence that the failure fraction is less than 0.01. For instance, one observed failure out of 480 particles and 80 observed failures out of 9500 particles are both sufficient conditions.

Knowledge of the 95% confidence level curve allows qualification of the various HTGR fuel types with a system such as IMGA. For this application, fuel particles are fed through the system individually and the failed, not-failed decision is made for each particle. The intersection

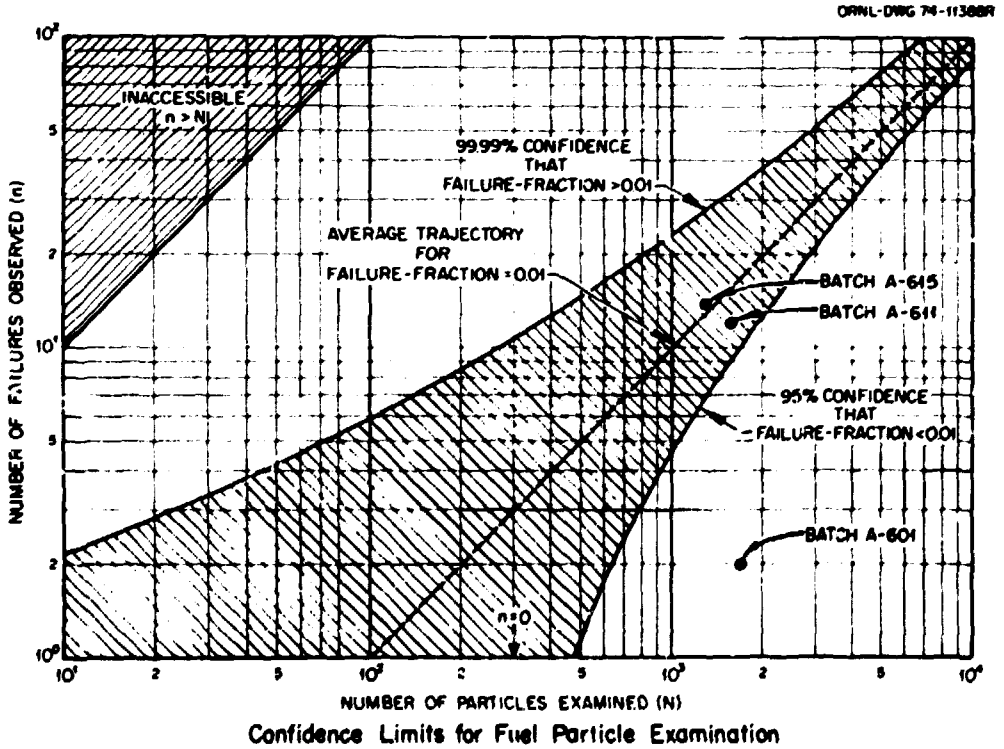

Confidence Limits for Fuel Particle Examination

Fig. 8. Statistical Considerations Require that to Satisfy the 95% Confidence Level that Failure Fraction is Less than 0.01 a Minimum of 300 Particles be Examined with no Observed Failed Particles.

at any point on the lower curve yields 95% confidence that the failure fraction is less than 0.01 and therefore demonstrates (with 95% confidence) that the design limit has been satisfied. Similarly, the intersection at any point on the line labeled "99.99% confidence that failure-fraction > 0.01" yields 99.99% confidence that the failure fraction exceeds 0.01. Although the 99.99% confidence was chosen arbitrarily for illustration, practical values should probably be fairly high to minimize the probability of rejecting a fuel that is actually acceptable. Figure 8 also illustrates that the minimum number of particles that must be examined, when no failures are detected, is 300 to establish with 95% confidence that the failure fraction does not exceed 0.01.

The extension of this theme for a failure fraction criterion of less than 0.005 is shown in Fig. 9. The figure has particular importance as it represents the present failure fraction limit of irradiated fuel particles, both fissile and fertile, with the exclusion of all fabrication defects.

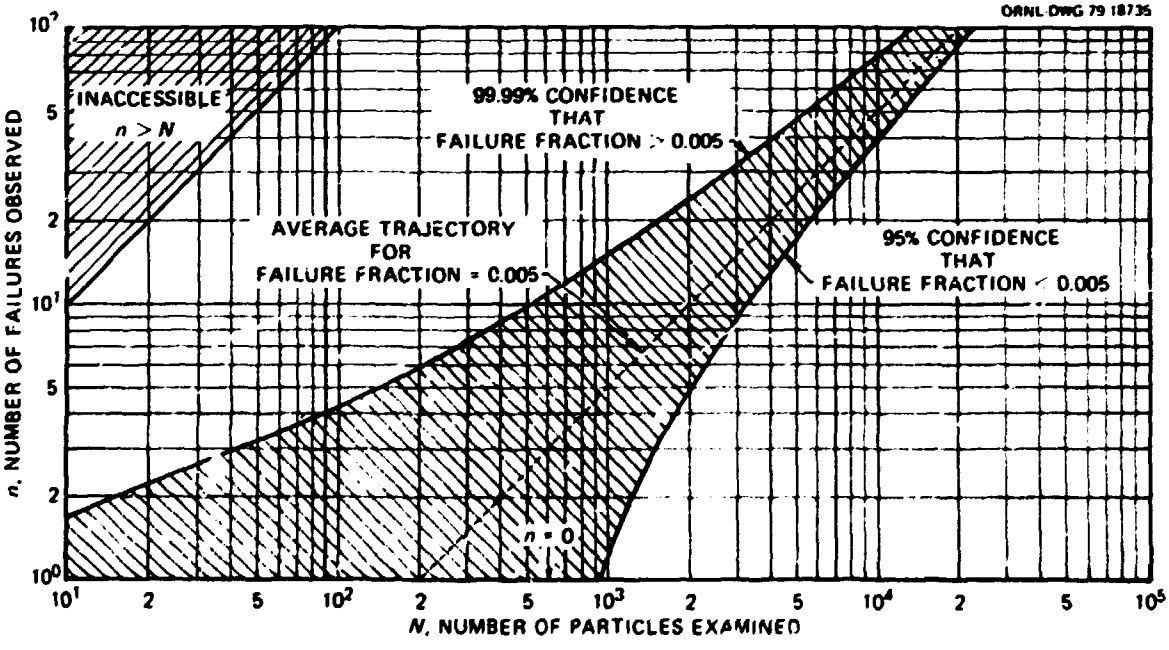

Fig. 9. Statistical Considerations Require that to Satisfy the 95% Confidence Level that Failure Fraction is Less than 0.005, a Minimum of 600 Particles be Examined with no Observed Failed Particles.

4.3 Statistics of the Gamma-Counting Process

To this point the assumption has been made that it is possible to establish with 100% confidence whether or not a particle is failed. However, when the failure criteria are based on the ratio of two fission product activities (e.g., Cs/Zr), as determined by gamma counting, then the statistics of the gamma counting must also be considered.

The ultimate aim for a system such as IMGA is to examine EOL HTGR fuel particles with failure fractions (fissile + fertile) of 1% to 0.01%. Thus, the misclassification of only one in thousands of particles can produce a quite large error in the failure fraction. By assuming normal distributions for the two fission products a good deal of insight into the problem can be gained, as the resulting distribution for the ratio can then be solved for analytically. Denoting the two fission product gamma counts by x and y, the distributions for the measured counts of a group of similar particles are:

$$P_x(x) = \exp[-(x - M)^2/2\sigma_x^2]/\sigma_x\sqrt{2\pi} \ , \tag{8}$$

$$P_y(y) = \exp[-(y - N)^2/2\sigma_y^2]/\sigma_y\sqrt{2\pi} \ , \tag{9}$$

where M and N are the mean values of x and y respectively and σ_x and σ_y are the standard deviations of the distributions, P_x and P_y. It can be shown that the distribution of the ratio, $R = y/x$, is given by

$$P(R) = \int_0^\infty P_x(t)P_y(Rt)t \ dt \approx \int_{-\infty}^\infty P_x(t)P_y(Rt)t \ dt \ . \tag{10}$$

Performing the indicated integration and defining $R_M = N/M$, $s_x = x/M$, $s_y = y/N$, and $s^2(R) = R^2s_x^2 + R_M^2s_y^2$, we obtain

$$P(R) = \frac{1}{\sqrt{2\pi}s(R)} \frac{R_M(Rs_x^2 + R_M s_y^2)}{s^2(R)} \exp[-(R - R_M)^2/2s^2(R)] \ . \tag{11}$$

The distribution for the ratio is seen to be a normal-like distribution with a maximum near $R = R_M$. The major difference is that it rises to the maximum more rapidly and falls from the maximum more slowly than a true normal distribution.

The problem of separating failed particles from unfailed particles can now be stated in the following terms. Let the main group of unfailed particles be characterized by the ratio R_g and failed particles by $R \leq R_b$, where $R_g > R_b$. In order to make an accurate determination of the failure fraction, the amount of mixing of the two groups must be kept to an acceptable minimum or:

$$\int_{-\infty}^{R_b} P(R_g)dR_g \ll \text{failure fraction} . \tag{12}$$

In many, if not most, cases the above integral involves only a tail of the distribution $P(R_g)$. Since the normal approximation, being a low order expansion, is not accurate in the tails, more accurate (but less tractable) Poisson statistics should be applied. This was done and the results are shown in Fig. 10 for several different values of M with $N = M$. Considering the curve for $M = N = 1000$, we see that if $R_g = 1$ and $R_b = 0.8$ (20% Cs loss), then the probability of cross mixing is about 6×10^{-7}. In other words, less than one particle in a million will be erroneously classified. For M and N greater than 1000, results obtained using the normal approximation (Gaussian distribution) nearly coincide with those obtained from the Poisson distribution.

Figure 10 illustrates that the probability that mixing errors occur decreases as the total number of counts for individual peaks increases. When counting rates are sufficiently high, then the counting time becomes the important factor in improving individual peak statistics. This point is illustrated in Fig. 11 for two counting times, 3 and 30 s on 1225 measurements[17] of ^{137}Cs and ^{95}Zr on a single HT-31 driver particle taken at a fixed geometry. As can be seen, the normalized $^{137}Cs/^{95}Zr$ ratio distributions are quite different for the two counting times. With a counting time of 3 s, the distribution is broad, ranging from 0.65 to

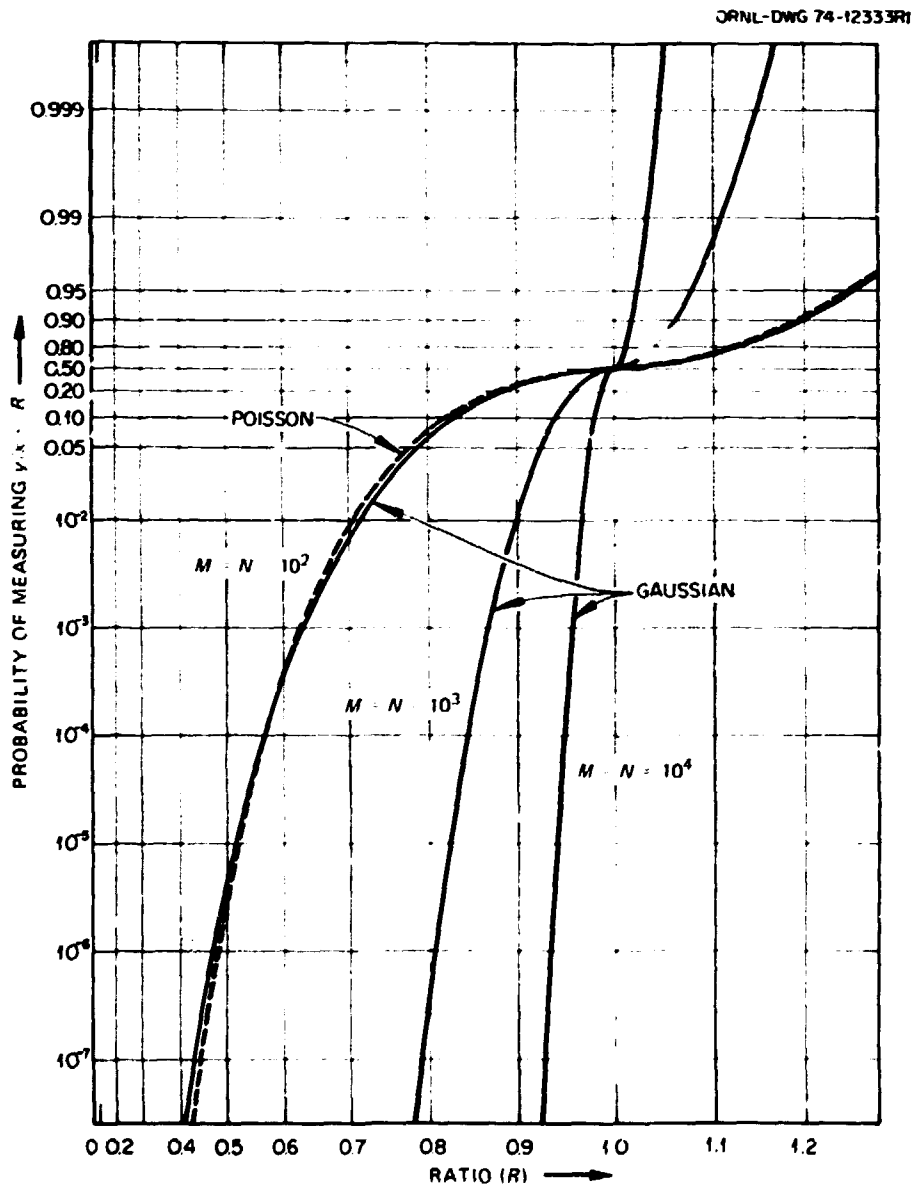

Fig. 10. The Probability for Misclassification of a Particle Based on the Ratio of Two Statistical Fission Product Activities Decreases as the Total Number of Counts Detected Increases. For $M = N > 1000$ the Poisson curves coincide with the Gaussian curves.

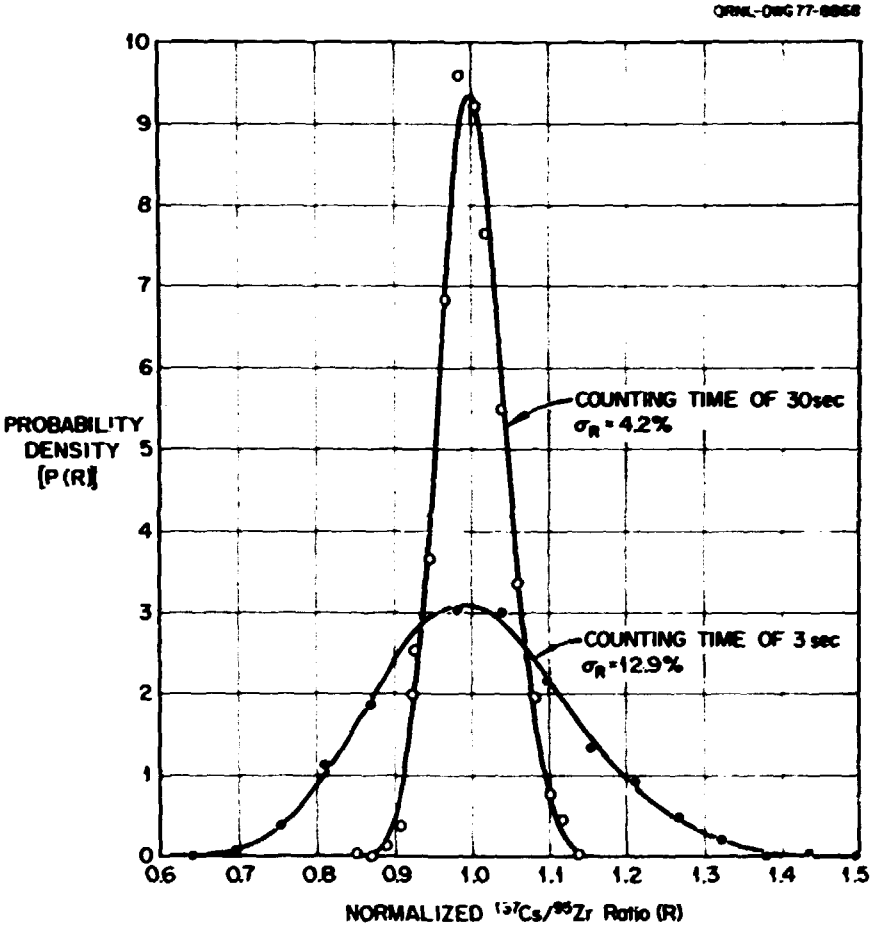

Fig. 11. Gamma Counting Statistics can Produce Significant Mixing Errors when Individual Peak Statistics Are Poor. Statistics can be improved by increasing the total counting time.

1.50; individual peak statistics are 10.06% for ^{137}Cs and 7.85% for ^{95}Zr. With a counting time of 30 s the distribution is much sharper, ranging from 0.85 to 1.15; individual peak statistics are 3.34% for ^{137}Cs and 2.59% for ^{95}Zr.

Failure fraction determinations based on one or the other of these $^{137}Cs/^{95}Zr$ distributions can lead to conflicting conclusions and are a result of mixing errors. In the previous discussion a ratio of 0.8 (20% cesium loss) was considered failure. If this criterion is applied here, the area under the distributions with ratios less than 0.8 represents the number of failed particles detected. At a 30 s counting time this area represents less than 1 failed particle; for 3 s this area represents about

39 failed particles. Applying failure fraction criteria of less than 1% at 95% confidence level (described in Fig. 8), the conclusion reached for 3-s results is that irradiation performance was poor. However, this result is erroneous because of mixing errors that have resulted from poor individual peak statistics. The correct conclusion, given by 30-s results, is that irradiation performance was good and exceeded failure fraction requirements based on values presented in Fig. 8.

Measurements made on irradiated fuel particles have demonstrated that data can easily be accumulated in the full energy peak of ^{137}Cs at rates up to 500 counts/s and in the two zirconium peaks at rates up to 300 counts/s. While the absolute accumulation rates depend on the number of effective full power days (EFPD), burnup, and cooling time, the time required by IMGA to make the failed, not-failed decision will clearly be of the order of 10 s.

5. IMGA OPERATION

Irradiated coated particles were first introduced into the IMGA cubicle in February 1977. Since that time more than 10^6 particles have been cycled through the automated particle handler during routine analyses. During this period each subsystem was thoroughly evaluated. Initial design flaws have been corrected and, where needed, new components designed, tested, and installed. The IMGA was built such that the cell containing the particle handler could be decontaminated whenever required. This feature was utilized whenever component redesign and installation were necessary.

5.1 Operational Software

The operational software for the Tennecomp Systems, Inc., TP-5000* pulse height analysis system is written in PDF machine language and was purchased with the system.

*Trademark of Tennecomp Systems, Inc.

5.2 Interpretive Software

The interpretive software for the IMGA system was developed at ORNL in a language known as TIL* (Tennecomp Interpretive Language), which is a version of FOCAL-11. The software is complete, fully tested, and operational.

5.2.1 Main Examination Program: FAILFRAK

The main examination program is called FAILFRAK and is used to control the entire operation of the IMGA system. The major functions of the program are to initialize and operate the particle handler, control particle-spectrum acquisition, analyze spectra, transfer data to mass-storage devices, and segregate particles according to a user-supplied criterion. Figure 12 is a flow diagram describing the features of the FAILFRAK program that are normally utilized in the individual particle examinations. A thorough description of the program is contained in the *IMGA Operating Manual*.[18]

Particular features of FAILFRAK that provide for efficient analysis of a multi-particle-type population of irradiated fuel are:

- computer-controlled energy-range selection;
- ability to select individual peaks in energy range of interest while ignoring others;
- inert particle detection capability, which reduces total operating time;
- ability to classify and analyze both fissile and fertile particle types during the same run.

The successful execution of this program results in two types of output: (1) physical segregation of particles according to the user-supplied selection criterion and (2) a series of library data files consisting of a setup file, one or more particle data set files, and a termination file.

5.2.2 Data Analysis Program: CRUNCH

The actual assembly of statistical results on fission product retention properties is handled in a separate program, CRUNCH, which utilizes

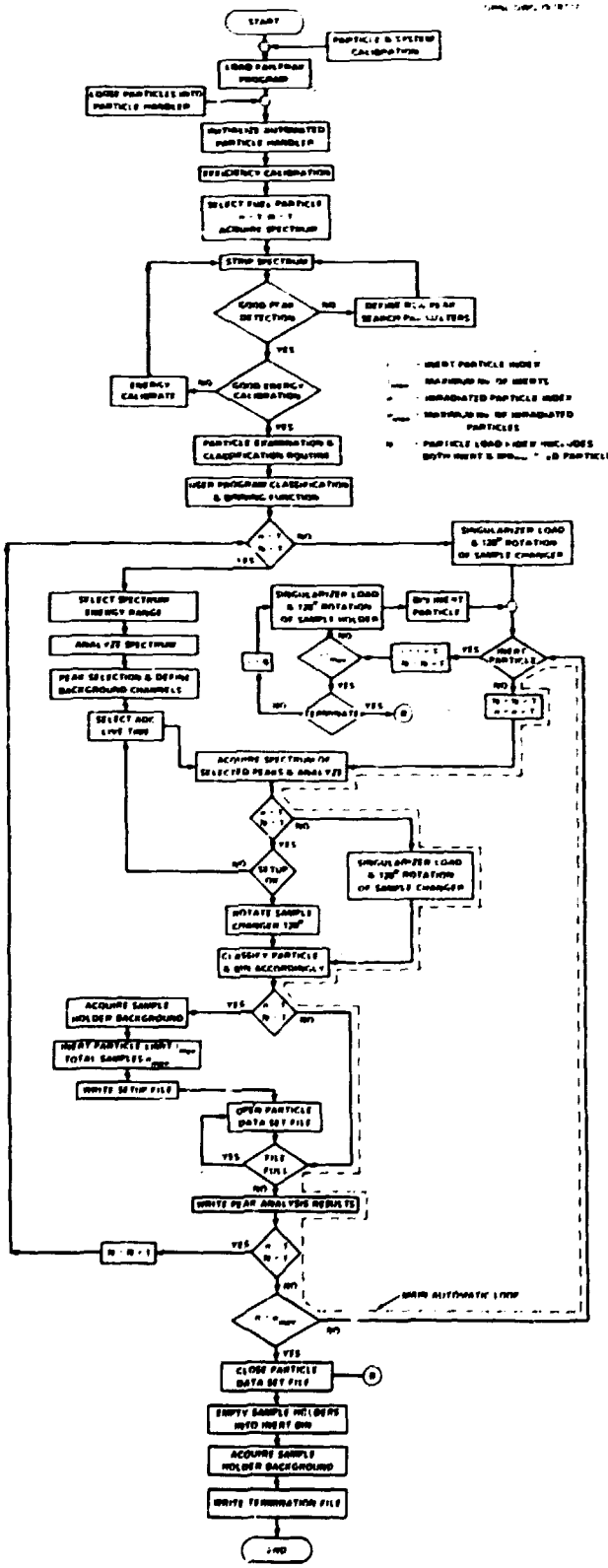

Fig. 12. Flow Diagram of IMGA Fuel Particle Examination Program FAILFRAK.

the library data files generated by the FAILFRAK program. This program analyzes both fissile and fertile particle data simultaneously while rejecting data from coating fragments or multiple loads (spectra acquired from two or more particles at the same time). Three basic functions are supplied by CRUNCH:

1. It lists the setup data file, which fully characterizes what particle examinations and classifications were done and how they were done.

2. It creates histograms of specific fission and activation product activities as well as user-defined ratios of these fission and activation products (i.e., $^{137}Cs/^{95}Zr$ and $^{134}Cs/^{137}Cs$). Use of parity functions enables generation of separate fissile and fertile histograms and allows removal of unwanted data sets.

3. It provides semirandom access to particle data sets.

A detailed description of the CRUNCH program and a step-by-step example of its use are reported elsewhere.[18]

6. DEMONSTRATION OF IMGA EVALUATION

The fuel selected for this demonstration was fuel rod C-3-1 irradiated in the OF-2 experiment.[19] This fuel rod achieved an average fast fluence of $8.9 \times 10^{25} n/m^2$ [>29 fJ (0.18 MeV)] in the Oak Ridge Research Reactor (ORR) over a period of 8440 h at 30 MW full reactor power.[20] The peak operating temperature was 1350°C and the average operating temperature was near 1250°C. The fuel rod contained fissile particle batch A-611, a 15%-converted weak-acid-resin-derived (WAR) kernel with a Triso-coating, and the fertile particle batch J-481, a ThO_2 kernel with an LTI Biso-coating. The fissile particle achieved a total burnup of about 75% FIMA and the fertile particle about 4.3% FIMA. The fuel rod was fabricated by the slug-injection process and contained, in addition to fuel particles, both shim and inert particles.

6.1 Deconsolidation Process

Fuel rod C-3-1 was electrolytically deconsolidated[14] to obtain loose fuel particles for the IMGA system. As with all deconsolidated fuel rods,

a sample of the electrolyte used in the process was submitted for chemical analysis of uranium and thorium contents. The results showed 1 mg/liter Th and 0.3 mg/liter U. These values are actually at the minimum detection limit of the apparatus and represent less than one particle at indicated burnup. These data indicate that the electrolytic deconsolidation process produced no additional particle failures from fuel rod C-3-1. The fuel particles, which include fissile, fertile, and inert, were shape separated from the shim particles and matrix debri and sent to the IMGA cubicle for analysis. This quantity of particles was then split into two portions by a random splitter, and one portion was introduced into the automated particle handler.

6.2 Examination of C-3-1 Fuel Particles

The IMGA system ran continuously for a period of nearly 100 h for the C-3-1 fuel particle examinations. In this period the system recorded a total of 13,374 particle loads. From this number, 1656 were classified as fissile, 3344 as fertile, and 8,374 as inert particles. The particles were subjected to a fissile-fertile-inert classification as well as a segregation within the fissile and fertile groups as to specific fission product activity ratios.

For each particle, 11 gamma peaks were selected from the total gamma-ray spectrum. The counting time for each fuel particle was 40 s of analog-to-digital converter live time; inert particles were detected in a fraction of a second. The 11 peaks recorded for each particle data set are described in Table 1; these data are for a typical fertile particle. Peaks 1 and 2, which are the K-shell fluorescent x rays from ^{232}Th ($K\alpha_2$ and $K\alpha_1$, respectively), were used to make the fissile-fertile particle split. The ratio of peak 3 to peak 4, $^{134}Cs/^{95}Zr$, was used to determine if particles had sufficient cesium. The ratio of peak 3 to peak 5, $^{134}Cs/^{137}Cs$, was used to determine if particles had lost an appreciable amount of fission gas. These five peaks, 1 through 5, were used in the classification of particles and the remaining 6 were recorded for later use in determining actual fission product retention characteristics of the particles. Along with the 11 gamma peaks and their associated

Table 1. Selected Peaks from Gamma-Ray Spectrum on One Fertile Particle[a] from OF-2 Fuel Rod C-3-1 During IMGA Analysis

Peak	Isotope	Energy		Standard Deviation	Source
		(fJ)	(keV)	(%)	
1	^{232}Th	14.42	90.0	4.33	$K\alpha_2$ x ray excited from ^{232}Th
2	^{232}Th	14.98	93.5	3.55	$K\alpha_1$ x ray excited from ^{232}Th
3	^{134}Cs	96.88	604.7	1.26	Activation product from $^{133}Cs(n,\gamma)$
4	^{95}Nb	122.70	765.8	1.94	Daughter of fission product ^{95}Zr
5	^{137}Cs	106.00	661.6	1.17	Fission product
6	^{144}Ce	21.39	133.5	0.94	Fission product
7	^{106}Ru	82.00	511.8	7.14	Fission product
8	^{106}Ru	99.[illegible]	621.8	13.11	Fission product
9	^{95}Zr	116.[illegible]	724.2	4.60	Fission product
10	^{95}Zr	121.27	756.9	4.35	Fission product
11	^{134}Cs	127.50	795.8	1.65	Activation product from $^{133}Cs(n,\gamma)$

[a]Fertile particle batch J-481.

counting statistics, the time during the examination when each spectrum was accumulated was also recorded to make decay time corrections on each particle data set. This is necessary to eliminate histogram peak broadening due to decay that occurs during the IMGA run.

The fissile-fertile histogram is shown in Fig. 13. The histogram, 50 channels wide, was formed by summing peaks 1 and 2 and then plotting the number of data sets whose sum for these peaks occurs between each channel limit. This figure shows excellent separation between fissile and fertile populations, approximately 28 channels. The area at the far left represents 1656 fissile particle loads and the area on the right represents 3344 fertile particle loads.

As indicated earlier, fuel particles were classified by a user-supplied criterion. The classification criterion had the sequence shown in Fig. 14. First we determined whether a coating fragment or particle

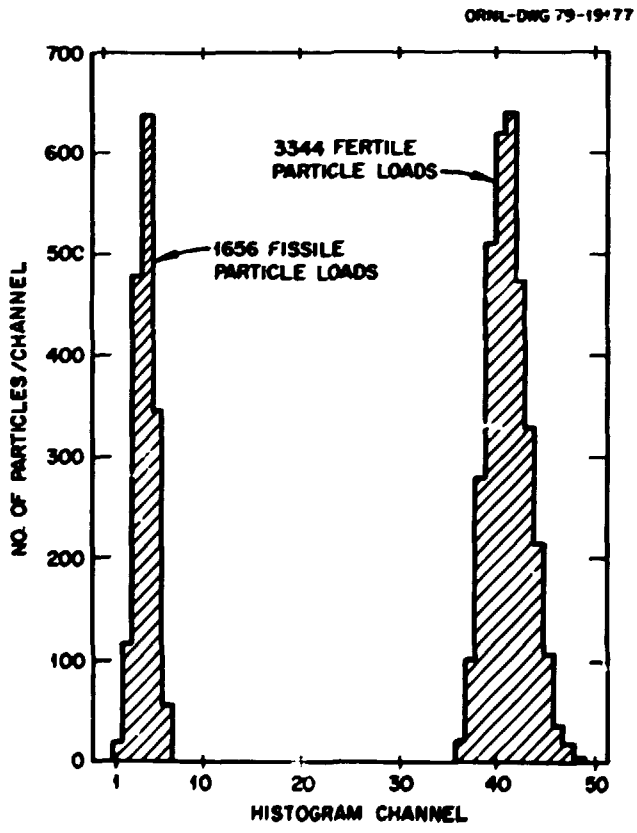

Fig. 13. Fissile-Fertile Particle Split Histogram from IMGA Examination of Particles from OF-2 Fuel Rod C-3-1. A total of 5000 fuel particles and 8374 inert particles were classified.

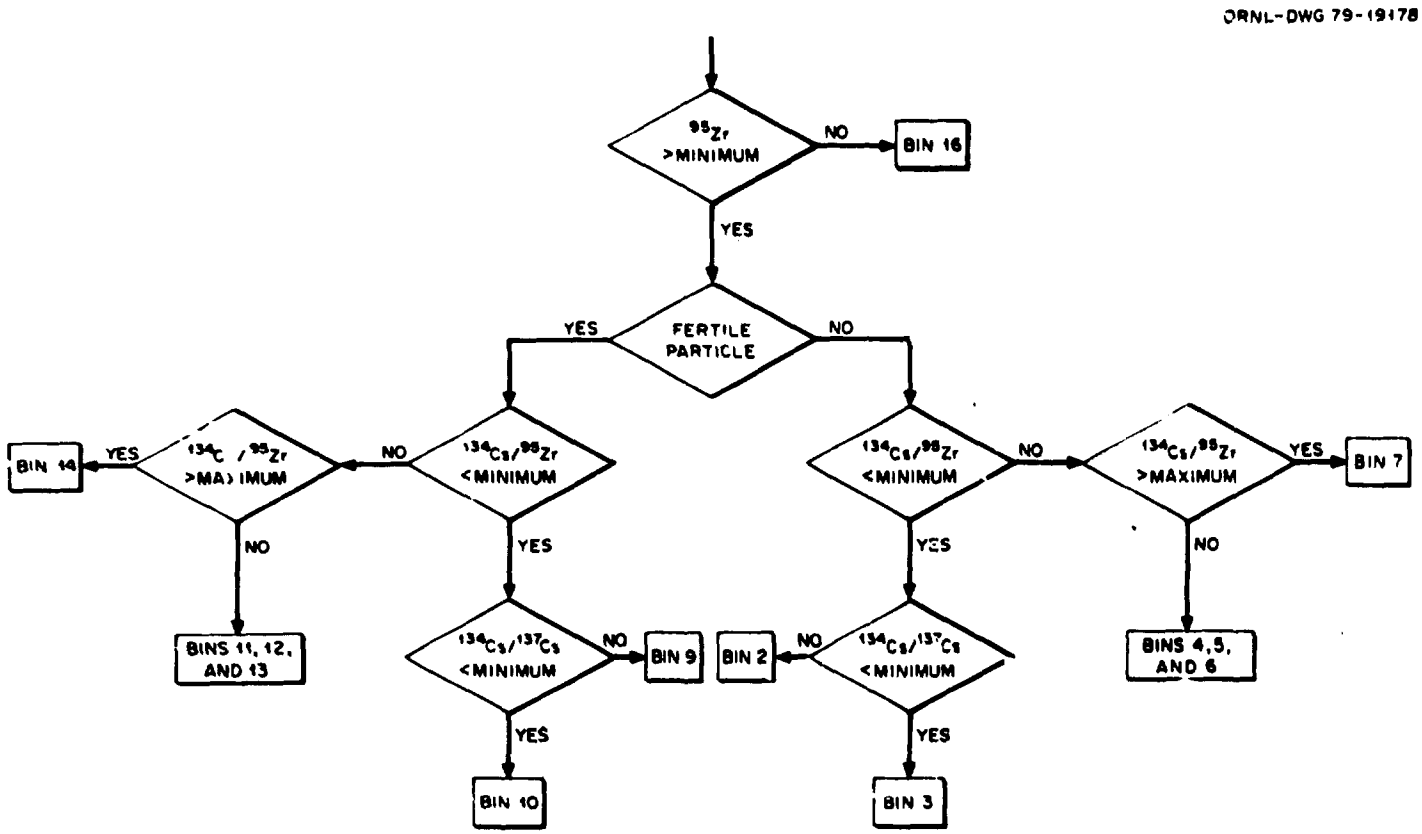

Fig. 14. Classification Criteria Used in the IMGA Examination of Fissile and Fertile Particles from OF-2 Fuel Rod C-3-1.

had been detected. If it was a coating fragment, it was put into bin 16; if not the execution was continued. Next the fissile-fertile classification was made. When the particle type was determined activity ratios were compared with minimum values. (Minimum values were selected from a "pre-run," which examined 200 particles on which minimum acceptable activity ratios were determined. This is a standard procedure that is carried out on all IMGA analyses.) The same type of comparisons were made for fissile and fertile particles. The activity ratio $^{134}Cs/^{95}Zr$ from peaks 3 and 4 was compared with a minimum acceptable value. If less than this value a $^{134}Cs/^{137}Cs$ comparison was made. If both $^{134}Cs/^{95}Zr$ and $^{134}Cs/^{137}Cs$ activity ratios were low the particle was put into bin 3 if fissile, bin 10 if fertile. If only the $^{134}Cs/^{95}Zr$ was low the particle was put into bin 2 if fissile, bin 9 if fertile. If $^{134}Cs/^{95}Zr$ was equal to or greater than the minimum value, a check was made if it was within the normal range. If within normal range the particle was put into bin 4, 5, or 6 if fissile, bin 11, 12, or 13 if fertile. If above the normal range, the particle was put into bin 7 if fissile, 14 if fertile. All inert particles were put into bin 18, 19, or 20. Table 2 shows the contents of the 20-bin collector after examination along with an explanation of the classification for each binning position.

The results of the classification on 1656 particles examined from fissile particle batch A-611 are: 6 had low $^{134}Cs/^{95}Zr$ ratios and were separated from the main distribution; 12 had low $^{134}Cs/^{95}Zr$ ratios and in addition low $^{134}Cs/^{137}Cs$ ratios and were also separated from main distribution. The remaining 1638 particles were classified as good. The classification of 3344 particles examined from fertile batch J-481 showed all as good particles. The apparent discrepency of two in the actual recorded number of fertile particles examined was due to a programming error at the beginning of examination run and represent "no-loads" that were put into one of the fertile bins. This programming error has subsequently been corrected.

6.3 Data Analysis of C-3-1 Fuel Particles

The first priority of the data analysis was to examine each data set and discard those that were not representative; for example, coating

Table 2. Classification of Fuel Particles from OF-2 Fuel Rod C-3-1 During IMGA Examination

Bin	Particle Type	Number of Particles	Classification
1		0	Not used
2	Fissile	6	Low $^{134}Cs/^{95}Zr$
3	Fissile	12	Low $^{134}Cs/^{95}Zr$ and $^{134}Cs/^{137}Cs$
4	Fissile	584	Good fissile particles
5	Fissile	527	
6	Fissile	527	
7	Fissile	0	High $^{134}Cs/^{95}Zr$
8		0	Not used
9	Fertile	0	Low $^{134}Cs/^{95}Zr$
10	Fertile	0	Low $^{134}Cs/^{95}Zr$ and $^{134}Cs/^{137}Cs$
11	Fertile	1131	Good fertile particles[a]
12	Fertile	1097	
13	Fertile	1118	
14	Fertile	0	High $^{134}Cs/^{95}Zr$ activity ratio
15		0	Not used
16	Fragment	0	Coating fragment
17		0	Not used
18	Inert	2770	Inert Particles
19	Inert	2791	
20	Inert	2811	

[a] Actual number of fertile data sets was 3344, not 3346 as indicated here. The reason for the discrepency of two was a programming error.

fragments or double loads consisting of a fissile and fertile particle being examined together. This was done and no discrepancies other than two "no loads" classified as fertile were noted.

A particle's ability to retain its fission products was determined by considering the activity ratios of $^{134}Cs/^{95}Zr$, $^{137}Cs/^{95}Zr$, $^{144}Ce/^{95}Zr$, and $^{134}Cs/^{137}Cs$. The reasons for selecting these ratios were discussed in Sect. 3.2. From Table 1, peaks 3 and 11 were combined to arrive at the total activity of ^{134}Cs. Peaks 4, 9, and 10 were combined to arrive at the total activity of ^{95}Zr. All data were corrected to a common analysis time for the OF-2 fuel (June 20, 1977). The actual time between removal of fuel from the ORR and this analysis was 511 d. Table 3 describes the results of the data analysis of OF-2 fuel rod C-3-1. Here minimum, maximum, and mean values for each isotope and each activity ratio are given for both fissile and fertile populations.

6.3.1 Fissile Particle Batch A-601

Figure 15 describes the activity ratios for the IMGA examination and data analysis on 1656 fissile particles ($^{134}Cs/^{95}Zr$ is not shown as it has results similar to those for $^{137}Cs/^{95}Zr$). Data are shown in histogram form from which the following results were obtained:

1. As determined by the $^{137}Cs/^{95}Zr$ ratio 18 particles have significantly* low inventories of cesium. Mean value of this ratio is 1.741, with a minimum of 0.011 and a maximum of 2.027. The standard deviation of the ratio over the population is 9.53%.

2. Of the 18 particles in 1 having low cesium inventories, 12 also show loss of fission gas by significantly* low $^{134}Cs/^{137}Cs$ ratios. Mean value of the ratio is 1.727 with a minimum of 0.473 and a maximum of 1.846. The standard deviation of the ratio over the population is 3.83%.

3. No particles had lost a significant* amount of rare earth fission product cerium as determined by the $^{144}Ce/^{95}Zr$ ratio. Mean value of the ratio is 12.46 with a minimum of 11.22 and a maximum of 14.02. The standard deviation over the population was 3.73%.

---

*Activity ratios that are at least 3 standard deviations less than the mean ratio of the population.

Table 3. Results of Data Analysis of OF-2 Fuel Rod C-3-1

Isotope or Activity Ratio	Activity,[a] Bq			Standard Deviation (%)
	Minimum	Maximum	Mean	
	1656 Fissile Particles			
^{95}Zr	1.808 E+6	3.478 E+6	2.585 E+6	12.51
^{134}Cs	4.389 E+4	1.075 E+7	7.792 E+6	15.14
^{137}Cs	2.842 E+4	6.046 E+6	4.498 E+6	14.87
^{144}Ce	2.335 E+7	4.213 E+7	3.216 E+7	11.71
$^{134}Cs/^{95}Zr$	0.018	3.618	3.018	10.35
$^{137}Cs/^{95}Zr$	0.011	2.027	1.741	9.53
$^{144}Ce/^{95}Zr$	11.219	14.015	12.459	3.73
$^{134}Cs/^{137}Cs$	0.472	1.846	1.727	3.83
	3344 Fertile Particles			
^{95}Zr	2.880 E+6	4.041 E+6	3.323 E+6	5.28
^{134}Cs	1.551 E+6	2.291 E+6	1.854 E+6	6.89
^{137}Cs	1.782 E+6	2.524 E+6	2.091 E+6	5.46
^{144}Ce	1.486 E+7	1.985 E+7	1.688 E+7	5.27
$^{134}Cs/^{95}Zr$	0.507	0.610	0.558	3.07
$^{137}Cs/^{95}Zr$	0.580	0.673	0.629	2.25
$^{144}Ce/^{95}Zr$	4.731	5.477	5.083	2.05
$^{134}Cs/^{137}Cs$	0.824	0.957	0.887	2.37

[a] Only isotope activity is given in becquerels; activity ratios are dimensionless.

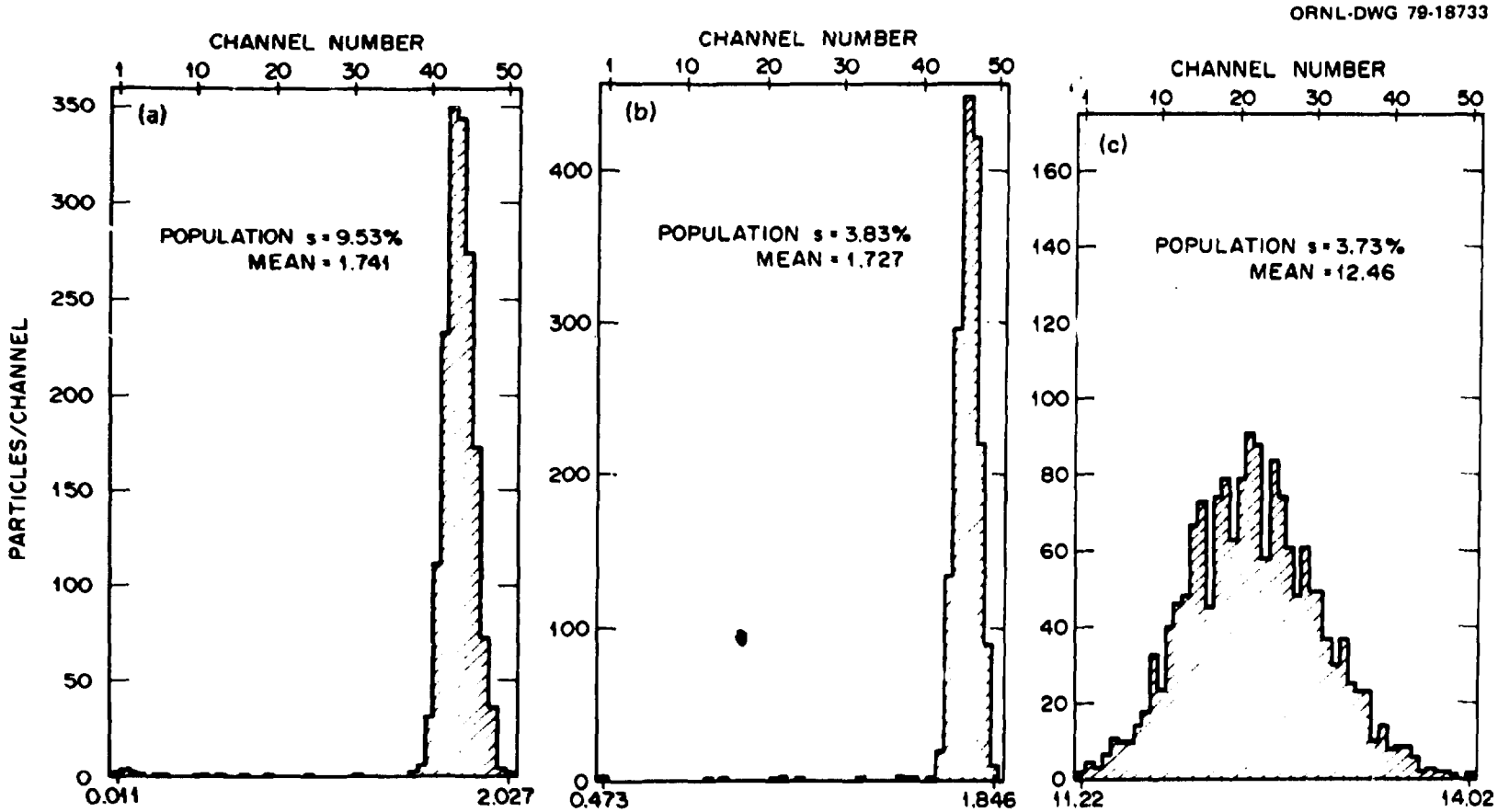

Fig. 15. Activity Ratios of (a) $^{137}Cs/^{95}Zr$, (b) $^{134}Cs/^{137}Cs$, and (c) $^{144}Ce/^{95}Zr$ Determined on 1656 Fissile Particle Examinations on WAR Particle Batch A-611. Fuel was irradiated in OF-2 experiment at 1250 ± 100°C at an average fast fluence of 8.9×10^{25} n/m^2 and an average burnup of 75% FIMA. Histograms show (a) 18 particles with significantly low $^{137}Cs/^{95}Zr$ ratios, (b) 12 particles with significantly low $^{134}Cs/^{137}Cs$ ratios, and (c) no particles with significantly low $^{144}Ce/^{95}Zr$ ratios.

The results indicate that 18 particles have broken SiC layers and have failed to retain the fission-product cesium. Of these 18 particles, 12 also had failed or permeable LTI layers that released fission gases. A comparison of these results and the requirements necessary to establish a failure fraction of 1% at a confidence level of 95%, Fig. 8, can be made. From the data 12 to 18 particles out of 1656 examined have failed to retain their gaseous and solid fission products. The minimum requirement for the 1% failure criterion is that only 9 failures be detectable out of 1656 examinations. Therefore, fissile particle batch A-611, from IMGA analysis of fuel rod C-3-1, does not have a failure fraction of 1% or less at the 95% confidence level.

6.3.2 Fertile Particle Batch J-481

Figure 16 describes the activity ratios for the IMGA examination and data analysis on 3344 fertile particles ($^{134}Cs/^{95}Zr$ ratio yields results similar to those for $^{137}Cs/^{95}Zr$ ratio). Data histograms indicate no significant* loss of cesium based on the $^{137}Cs/^{95}Zr$ ratio; no significant* loss of cesium based on the $^{137}Cs/^{95}Zr$ ratio; no significant* loss of fission gas xenon based on the $^{134}Cs/^{137}Cs$ ratio; and no significant* loss of cerium based on the $^{144}Ce/^{95}Zr$ ratio. A comparison of these results with requirements for 1% failure fraction, Fig. 8, indicates that minimum requirements have been met. Therefore, fertile particle batch J-481, from IMGA analysis on fuel rod C-3-1 from OF-2 irradiation experiment, does have a failure fraction less than 1% at the 95% confidence level.

Because no significant differences were observed with the fertile particles, a calculation using the CACA-2 computer code[21] in conjunction with the OF-2 neutronics data[22] was initiated to determine similar activity ratios as determined by IMGA analysis. An average fertile particle was considered in the analysis and the power history of the OF-2 experiment was modeled in the CACA-2 code. Calculated activity ratios

---

*Activity ratios that are at least 3 standard deviations less than the mean ratio of the population.

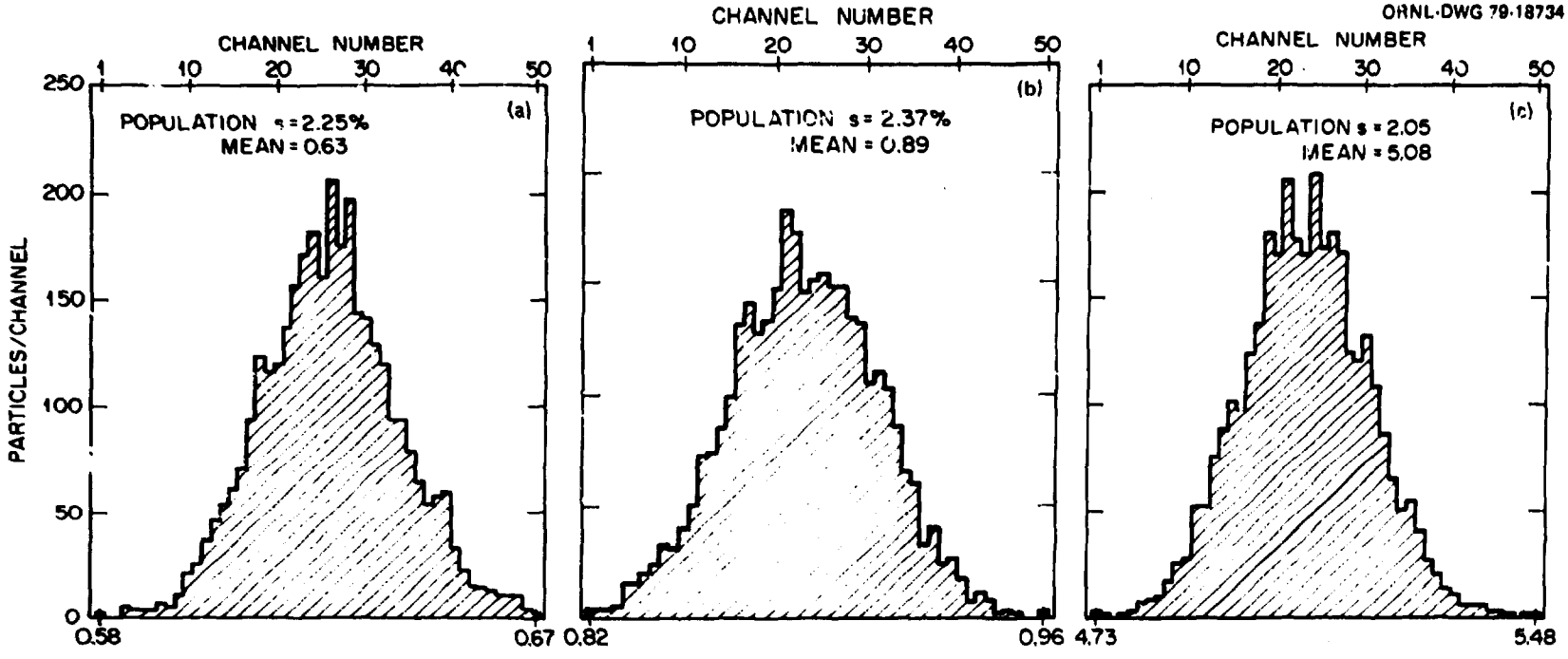

Fig. 16. Activity Ratios of (a) $^{137}Cs/^{95}Zr$, (b) $^{134}Cs/^{137}Cs$, and (c) $^{144}Ce/^{95}Zr$ Determined on 3344 Fertile Particle Examinations on Particle Batch J-481. Fuel was irradiated in OF-2 experiment at 1250 ± 100°C at an average fast fluence of 8.9×10^{25} n/m^2 and an average burnup of 4.3% FIMA. Histograms show no significantly low activity ratios for this particle batch.

were decay corrected to the same date as the IMGA analysis and the comparison between these data and the IMGA data is presented in Table 4. The comparison is excellent and provides further evidence of the good irradiation performance of the fertile particle batch J-481.

Table 4. Comparison Between Calculated and Measured Activity Ratios for Fertile Particle Batch J-481 of Fuel Rod C-3-1 of CR-2

Activity Ratio	IMGA Measurement	CACA-2 Calculation
$^{134}Cs/^{95}Zr$	0.558	0.551
$^{137}Cs/^{95}Zr$	0.629	0.620
$^{134}Cs/^{137}Cs$	0.887	0.889

7. SUMMARY

The Irradiated-Microsphere Gamma Analyzer System (IMGA) described in this report is now an integral part of the postirradiation evaluation of HTGR coated particle fuel at ORNL. The system physically consists of a high-resolution gamma-ray spectrometer, a computer-based analyzing system, and an automated remote particle handler. These three components and their interfaces have been integrated into a sophisticated and versatile system and demonstrated to be efficient, reliable, and accurate. Some of the important and unique features of the IMGA system are summarized below:

1. The primary purpose is to assess the fission product retention capabilities of irradiated HTGR coated particle fuel in order to verify fuel product performance specifications as to failure fraction requirements. This assessment is accomplished by performing a nondestructive quantitative analysis of important fission products to determine defective or broken coatings. This method preserves the fission-product inventory and distribution within particles as they were at end of irradiation.

2. It is an automated system that can examine a large population of irradiated coated particle fuel, segregate those particles where poor

performance is indicated, and perform a complete data analysis. Failed-nonfailed decisions are based upon a user-supplied criterion. Actual failure fractions are based upon the activity ratio of a volatile fission product to a nonvolatile one, such as $^{137}Cs/^{95}Zr$. This method eliminates uncertainties associated with variations in kernel size and heavy-metal loading. Failed particles are physically separated from nonfailed particles to allow further examination by other detailed PIE techniques to determine failure mechanisms.

3. Irradiation performance assessment is based upon the examination of each particle from a statistically significant population size. The IMGA data, n failures out of N examinations, is accurately described by the binomial probability distribution model. By using this model, a mathematical relationship between IMGA data (n,N), failure fraction, and confidence level has been developed.

4. Examination of both fissile and fertile particle types is possible during the same run; inert particle detection capability is also present. Coating type is immaterial; both Biso- and Triso-coatings are equally well evaluated. Once set up, the IMGA system can run without operator attendance for the long periods of time necessary for examination of population sizes required for verification of failure fractions in the 10^{-2} to 10^{-4} range.

8. ACKNOWLEDGMENTS

The authors wish to acknowledge the efforts of many people who made significant contributions in the planning, design, and implementation of the IMGA system. We would like to acknowledge F. J. Homan for his support and planning, which have allowed us to pursue the installation of the IMGA system; E. L. Long, Jr., whose original ideas have taken shape in the IMGA system; M. G. Willey of the Experimental Engineering Division for his design work on the automated particle handler and the helpful discussions on its operation. We would also like to acknowledge S. E. Disluke and W. P. Parsley of the High Radiation Level Examination Laboratory (HRLEL) for their design and implementation of the IMGA cubicle, the stereomicroscope stage, and their associated equipment. Also, our appreciation goes

to E. L. Ryan of the Fuels Evaluation Group and G. A. Moore of the HRLEL for their operation of the system and their patience during implementation of hardware and software. We would like to thank R. J. Lauf and E. L. Long, Jr., for their technical review of this report. The authors acknowledge those who assisted in the preparation of this report: S. Peterson for technical editing and S. G. Frykman for makeup and typing.

9. REFERENCES

1. T. D. Gulden and H. Nickel, "PREFACE: Coated Particle Fuels," *Nucl. Technol.* 35: 206–13 (September 1977).
2. R.L.R. Lefevre and M.S.T. Price, "Coated Nuclear Fuel Particles: The Coating Process and its Model," *Nucl. Technol.* 35: 263–78 (September 1977).
3. D. P. Harmon and C. B. Scott, *Development and Irradiation Performance of LHTGR Fuel*, GA-A-13173 (October 1975).
4. C. L. Smith, *Fuel Particle Behavior Under Normal and Transient Conditions*, GA-A-12971 (GA-LTR-15) (October 1974).
5. K. H. Valentine and E. L. Long, Jr., "Fuel Particle Inspection with an Irradiated Microsphere Gamma Analyzer," *Trans. Am. Nucl. Soc.* 22: 213 (1975).
6. M. J. Kania et al., "Irradiated Microsphere Gamma Analyzer," *HTGR Base-Technology Program Progress Report for July 1, 1975 through December 31, 1976*, ORNL-5274, pp, 351–58 (November 1977)
7. F. J. Homan, E. L. Long, Jr., T. B. Lindemer, R. L. Beatty, and T. N. Tiegs, *Development of a Fissile Particle for HTGR Fuel Recycle*, ORNL/TM-5602 (December 1976).
8. E. Balthesen et al., "HTGR Fuel Development and Testing," pp. 201–17 in *ANS Topical Meeting, Gas-Cooled Reactors: HTGR and GCFBR, May 7–10, 1974, Gatlinburg, Tennessee*, CONF-740501.
9. L. W. Graham et al., "HTR Fuel Development and Testing in the Dragon Project," pp. 218–56 in *ANS Topical Meeting, Gas-Cooled Reactors: HTGR and GCFBR, May 7–10, 1974, Gatlinburg, Tennessee*, CONF-740501.

10 P. L. Allen, L. H. Ford and J. V. Shennan, "Nuclear Fuel Coated Particle Development in the Reactor Fuel Element Laboratories of the U. K. Atomic Energy Authority," *Nucl. Technol.* 35: 246–53 (September 1977).

11. F. J. Homan and E. L. Long, Jr., *Irradiation Performance of HTGR Recycle Fissile Fuel,* ORNL/TM-5502 (August 1976).

12. Several articles on "Performance and Performance Modeling," *Nucl. Technol.,* 35: 343–454 (September 1977).

13. C. B. Scott, *Thermochemical Stability of Irradiated HTGR Fuel Particles,* GULF-GA-B-12409 (May 1, 1973).

14. T. N. Tiegs, E. L. Ryan, and M. J. Kania, *HTGR Fuel Rod Deconsolidation,* ORNL/TM-6426 (December 1978).

15. K. H. Valentine, "Statistical Basis for Failure Fraction Determinations," *HTGR Base-Technology Program Progress Report for January 1, 1974–June 30, 1975,* ORNL-5108, pp. 450–56.

16. M. Abramowitz and I. A. Stegun, eds., *Handbook of Mathematical Functions,* National Bureau of Standards Applied Math. Ser. 55, U. S. Government Printing Office, Washington, 1964, p. 944.

17. T. N. Tiegs, J M Robbins, R. L. Hamner, B. H. Montgomery, M. J. Kania, T. B. Lindemer, and C. S. Morgan *Irradiation Performance of HTGR Fuel in HFIR Capsule HT-31,* ORNL-5510 (May 1979).

18. K. H. Valentine and M. J. Kania, *IMGA Operating Manual,* ORNL-6576 (August 1979).

19. K. R. Thoms and M. J. Kania, *Design, Fabrication, and Initial Operation of HTGR-ORR Capsule OF-2,* ORNL/TM-5459 (March 1977).

20. T. N. Tiegs and K. R. Thoms, *Operation and Postirradiation Examination of ORR Capsule OF-2: Accelerated Testing of HTGR Fuel,* ORNL-5428 (March 1979).

21. E. J. Allen, *CACA-2: Revised Version of CACA-A Heavy Isotopes and Fission Product Concentration Calculational Code for Experimental Irradiation Capsules,* ORNL/TM-5266 (February 1976).

22. J. F. Mincey, "OF-2 Neutronics Analysis," *HTGR Base-Technology Program Annu. Prog. Rep. Dec. 31, 1977,* ORNL-5412, pp. 121–27.